We are IntechOpen, the world's leading publisher of Open Access books Built by scientists, for scientists

4,800
Open access books available

122,000
International authors and editors

135M
Downloads

Our authors are among the

154
Countries delivered to

TOP 1%
most cited scientists

12.2%
Contributors from top 500 universities

WEB OF SCIENCE™

Selection of our books indexed in the Book Citation Index in Web of Science™ Core Collection (BKCI)

Interested in publishing with us?
Contact book.department@intechopen.com

Numbers displayed above are based on latest data collected.
For more information visit www.intechopen.com

9

Experimental Study on Acoustic Emission Characteristics of Concrete Failure Process Under Uniaxial Tension

Sheng-xing Wu, Yan Wang, Ji-kai Zhou and Yao Wang
Hohai University,
People's Republic of China

1. Introduction

Tension is the main mechanical form for concrete structures. The characteristics of concrete failure process under tension is an important part of concrete failure mechanism study [1], because tension of concrete is weak and concrete tends to crack. The post-peak softening response of concrete in direct tension seems primarily related to widening of a single crack, and the post-cracking resistance of concrete may be due to discontinuities in cracking at the submicroscopic level and to bridging of cracked surfaces by aggregates. Acoustic emission, a kind of real-time technique, detects microcrack activities in high sensitivity, thus it is widely used in concrete study. In this paper, the development and evolution of microcracks are studied by analyzing the AE signals of concrete specimens under uniaxial tension.

2. Testing procedure

2.1 Preparation of concrete specimens

Prism specimens in variable cross-section are prepared, and axial tensile force is applied using a steel bar with a diameter of 18mm pre-embedded in the specimen; the steel bar is connected with spherical hinge by thread. Dimension and the shape of concrete specimen are showed in Fig. 1. The materials used are Portland cement of type 32.5, river sand which has a fineness modulus of 2.6, crushed gravel (the maximum grain size is 16 mm). The corresponding content proportion of cement: sand: gravel: water is 1: 1.63: 2.66: 0.55. Concrete mixture is injected in steel molds, and then compacted using a vibrating table. The specimens are demolded the following day and sprayed in water tank for another 7 days, then cured at room temperature until they are tested. The age of specimens is about 150d.

2.2 Loading equipment

The tests are carried out in MTS 322 electro-hydraulic servo material test machine and FlexTest GT multi-channel controlling system. To obtain stable post-peak response of concrete specimens, the concrete specimens' own deformation is used as the control signal of closed-loop controlled test system. Unloading-reloading processes is performed at several points in the softening portion of the stress-strain curve in order to study the generation and development of microcracks, In addition, the stability of response in post-peak situation is

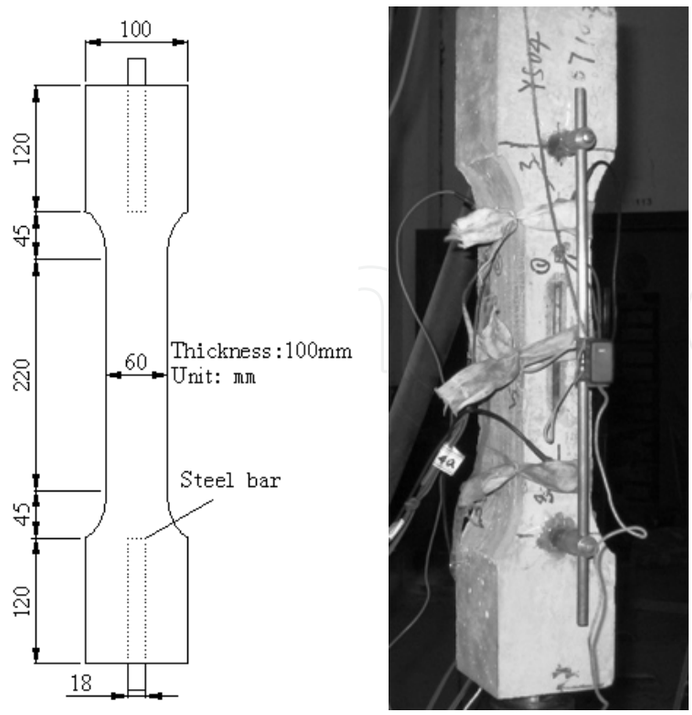

Fig. 1. Dimension and shape of concrete specimens

evaluated. Concrete fracture generally occurs in a particular region due to the development of a large number of micro-cracks. Then, visible cracks appear before the concrete fractures. Irrecoverable deformation occurs in this region, and strain softening phenomenon appears. irrecoverable deformations in this region are different to each other [2].Because the tension failure of concrete is the result of a single main crack growth, gradual failure can be obtained and instability near the peak load can be avoided if the opening of the crack is controlled in a closed-loop manner [3]. However, the final fracture position is unknown before testing for unnotched concrete specimen under direct tension. In order to find the microcrack localized region and to use the deformation of this region as control signal, longer distance for strain measurements are used in this study, see Tab. 1.

Series	Loading type	Transducers	Distance strain measurement
DT01	Monotonous	One broadband transducers	210mm
DT02	Unloading-reloading is performed at 2 points in the softening portion	One broadband and 4 resonant transducers (No. 1-5 in Fig. 2)	210mm
DT03	Unloading-reloading is performed at 3 points in the softening portion	One broadband and 5 resonant transducers (No. 1-6 in Fig. 2)	300mm
DT04	Unloading-reloading is performed at 4 points in the softening portion		275mm

Table 1. Loading types and of the transducer arrangements

2.3 AE data-acquisition system

Acoustic emission monitoring of concrete crack activity is performed using an advanced SAMOS ™ system supplied by PAC Ltd. AEwin ™ software is used to acquire and process the data. Both broadband and resonant transducers (Type: R6α, resonance frequency: 90kHz; and type: PAC-WD, Bandwidth 100kHz~1.0MHz) are attached to specimens using vaseline as coupling agent, then fixed using rubber band. The acoustic emission signals are amplified by a 40dB gain PAC-2/4/6 preamplifier, a Bandpass filter with a range of 10kHz～2.0MHz is used, the detail for the arrangement of the transducers is shown in Tab. 1.

Resonant transducers are used for 2D AE source location analysis, while the broadband transducer is used to analyze AE parameters. Considering the arrangement of strain measurement, such as strain gauges and extensometer, the arrangement of transducers are finally chosen, as shown in Fig. 2. The thresholds for broadband and resonant transducers are 35dB and 38dB respectively, which are just above the background noise level determined by preliminary tests.

2.4 Loading type

In order to get optimum results from the test, three preliminary tests are carried out, then the final test method is fixed. The results from these tests are not presented in this paper. The results of four concrete specimens are given, the series and loading tapes are shown in Tab. 1. Four strain gauges are attached to the middle of each side of specimens, and the data related to strain is acquired and stored by type DH5922 system and controlled by computer. Preloading of 5kN (about 0.83 MPa) is made in order to check if the deviation of four strain data from each side of the specimens is within 10%, then the extensometer is put on the highest strain side of the specimens.

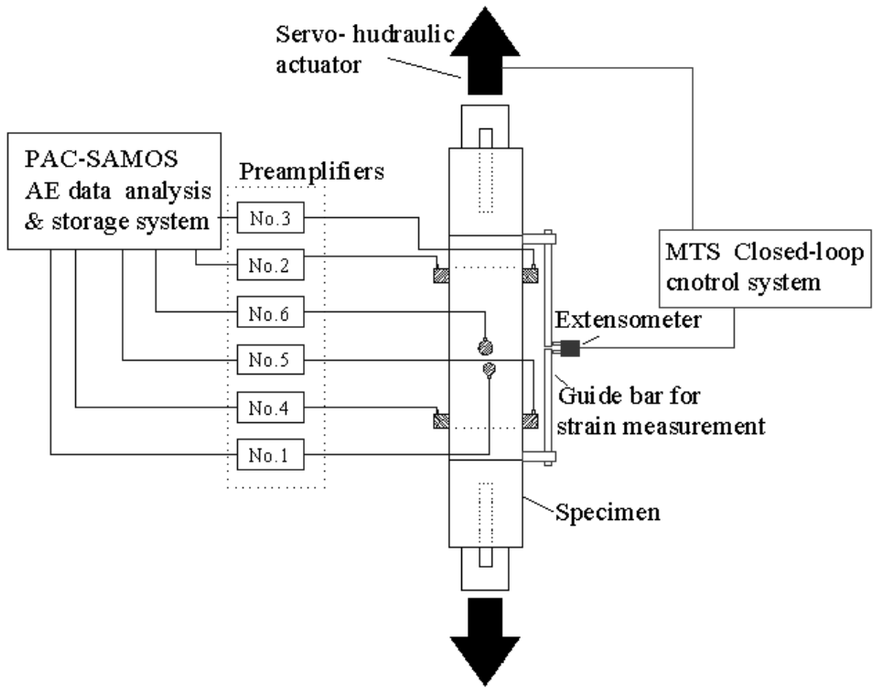

Fig. 2. Schematic diagram of the experimental set-up

3. Acoustic emission analysis

3.1 Acoustic emission parameters

The acoustic emission signal must be parameterized before analysis. The detection and measurement of an AE signal on a channel is called hit[4]. The AE hit parameters concerned in this paper are shown in Fig. 3. In the parameters, amplitude means the maximum AE signal excursion during an AE hit, count means the AE signal excursions over the AE threshold, the duration is defined as the time from the first threshold crossing to the end of the last threshold crossing of the AE signal from the AE threshold. Theoretical research[5, 6] showed that amplitude and duration are the best parameters to characterize the AE source mechanism. these two parameters are used in this paper, and accumulated AE hit number is also used to analyze the AE activity.

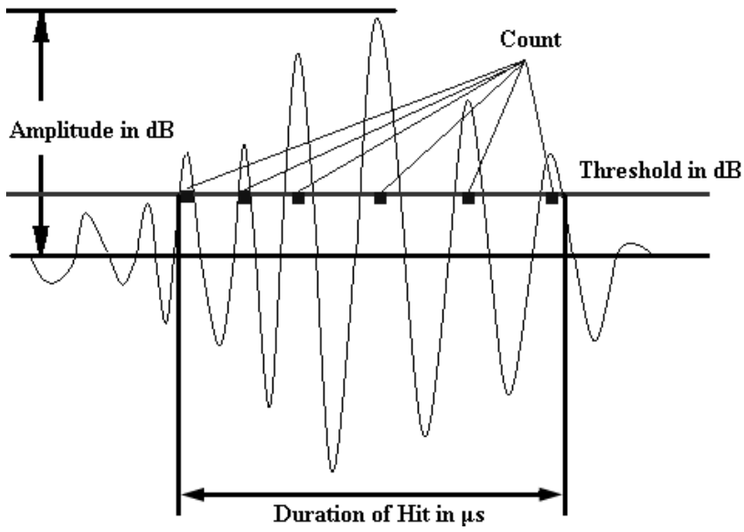

Fig. 3. AE signal parameters

3.2 AE source location

The AE source location can be deduced based on the differences among the arrival time at each transducers, In order to get a better estimate of the first arrival time, the AE signals are smoothed by using a band pass filter. The range of the band-pass filter is from 20 to 400 kHz. For a two-dimensional case, when the wave velocity is known, the calculated and observed value of the difference between the distance from transducer 1 to the AE source and the distance from transducer i to the AE source can be written as （d1－di）and Δt1i·Vp , respectively. The error between them can be written as:

$$e_{1i} = d_1 - d_i - \Delta t_{1i} V_p \tag{1}$$

Where: $d_1 = \sqrt{(x_e - x_1)^2 + (y_e - y_1)^2}$ is the distance from transducer 1 to the AE source; $d_i = \sqrt{(x_e - x_i)^2 + (y_e - y_i)^2}$ is the distance from transducer i to the AE source; xe, ye are the coordinates of the AE source to be determined; xi, yi (i=1, 2……n) are the coordinates of transducers; Δt1i is the difference of arrival time between transducer 1 and transducer i (i=2, 3, …, n); Vp represents the P-wave velocity.

In an ideal situation, the error expression e1i should be zero. However, in an actual experiment, errors always exist. To minimize the test error, in general, the idea of least square is introduced. The summation of individual errors can be expressed as Eq. (2), then different optimization methods can be employed to calculate the value of x, y and z.

$$e = \sum_{i=2}^{n} (e_{1i})^2 = \sum_{i=2}^{n} (d_1 - d_i - \Delta t_{1i} V_p)^2 \tag{2}$$

A new exhaust based method[7]is used in the paper: first, location zone is divided into mesh, second, the values of objective function of Eq. (2) in each node of the mesh are calculated and compared, then the coordinates are determined when the minimum value is found. The method evaluated the result by comparing the relative value of residual and needn't to set the initial value of iteration, so this method can improve the data utilization ratio.

4. Result and analysis

Tensile strength and the time at which the AE signal for each specimen appears are shown in Tab. 2.

Series	AE detected at	Tensile strength
DT01	1.19MPa (75%)	1.59MPa
DT02	1.67MPa (65%)	2.56MPa
DT03	0.96MPa (33%)	2.92MPa
DT04	0.64MPa (43%)	1.50MPa

Table 2. Tensile strength for concrete specimens

4.1 The description for each loading stages

The strain-stress curve and the accumulated AE hit number are shown in Fig. 4. Three continuous processes are used to describe the different stages of the development of microcracks and mechanical properties[8, 9]:

When the mechanical behaviour of the specimen corresponding to the different stages of cracking is considered, the following [10] is found if the test is performed at an imposed displacement rate (Fig. 4.)

4.1.1 Stage 1(O-A in Fig. 4): Random distribution of microcracks

Before the load reached 1.19MPa (about 72% ultimate stress), the axial stress increased successively with the strain, and is approximately proportional to the displacement, which is the elastic stage of concrete under Uniaxial tension. During this stage, the initial microcracks (due to the shrinkage of the cement paste blocked by the aggregates) are spread, and new microcracks form in the zones of lowest strength (paste-aggregate bond, for example) or in those zones where the local tensile stresses are higher (this is related to the fact that the aggregates and the cement paste have different mechanical characteristics). Because the AE activities are weak, the transducers on the specimen do not detect any AE signals during this stage.

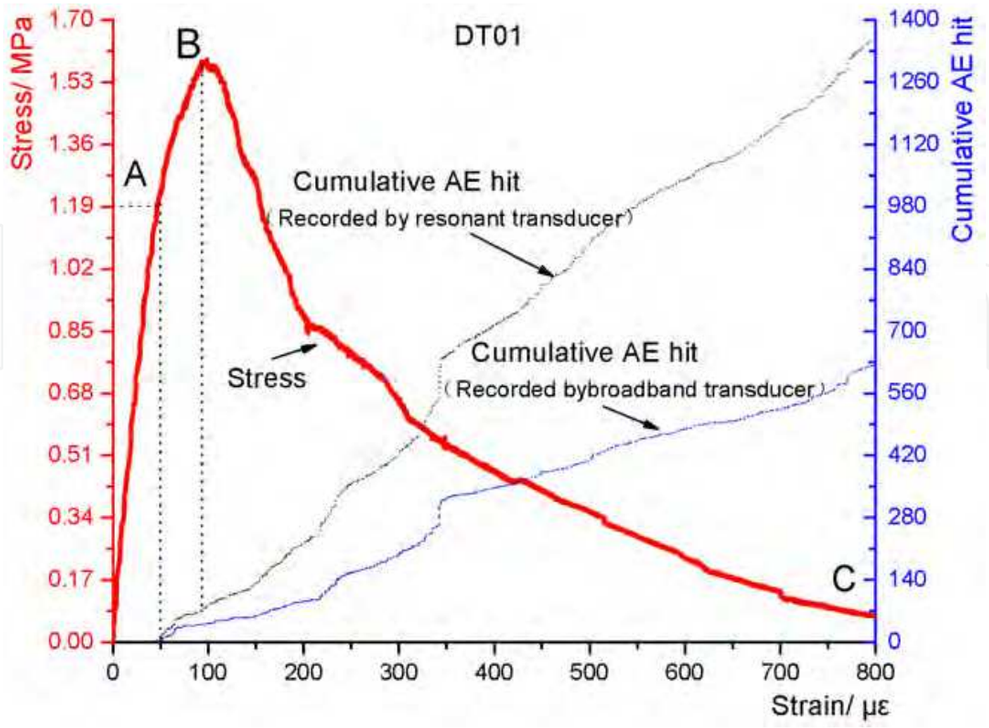

Fig. 4. Tensile stress and accumulated AE hit number versus strain

4.1.2 Stage 2(A-B in Fig. 4): Localization of microcracking

The elastic-plasticity deformation stage is from 1.19MPa to ultimate stress, and the stress-strain curve becomes a little nonlinear, AE signals higher than the threshold are generated in the further development process of microcracks, then recorded by AE system. During this process, the microcracks generated in the stage 1 developed further and macrocracks appeared, and at the same time, the micro-cracks localized phenomenon appeared, the emergence of macrocracks are the beginning of the third stage.

4.1.3 Stage 3 (B-C in Figure 4): Expansion of the macrocracks

When the tensile strength is realized , concrete specimen do not become faulty immediately, but cracking surface gradually been opened (though the naked eye may not be able to observe the cracks), with the increase of deformation the specimen still has some capacity, but the capacity declined rapidly, the stiffness of concrete specimen became smaller gradually and showed "softening" characteristics. At this stage, a stage before the macrocracks at this time continue to spread, performance for the cumulative impact of emissions continued to increase, leading to the loss of specimen bearing capacity.

In addition, as showed in fig. 4, when the strain reached about 350με, the curve of AE hit cumulative number showed suddenly increased for specimen DT01, this phenomenon may be related to the change of internal micro-structure of concrete specimen[10], and may also related to the localization of a single critical microcrack[11]. Sudden change in the stress-strain curves can not be seen clearly, its causes may be part of the micro-cracks in the location and not appear in the extended-distance side of the specimen surface. In contrast

with that in the specimen DT03, in the stress-strain curve shortly after the peak, there have also been the same phenomenon, and in the stress-strain curve has appeared on a sudden decline, due to the use of test closed-loop control technology, making micro-cracks in the unstable expansion to a certain degree of inhibition (otherwise for the sudden rupture, leading to the loss of specimens moment carrying capacity).

Thus, through monitoring the change of cumulative curve of AE hit, forecast and describe the development of instable microcrack can be achieved in real-time and high sensitivity.

4.2 AE Characteristics during unloading-reloading process in soften stage

During the test, performing limited times of unloading-reloading processes or changing the deformation rate will not affect envelope shape of the measured stress-strain curve, and the envelope of curve is identify to the curve which obtained from monotonous loading[12]. The unloading-reloading is performed at 3 and 4 points in the softening portion of the stress-strain curve in DT03 and DT04, respectively. It can be seen from Fig. 5, AE hit cumulative curve tend to be a horizon line during the processes of unloading-reloading, showed that there are no obvious AE activities in this processes. The relationship between AE count and axial stress are shown in fig. 6, it is also can be seen clearly that almost not AE activities are found in that processes. The above analysis is described from a qualitative point of view, the AE characteristics in the unloading-reloading processes will be analyzed referred to the stress and strain in the following parts.

4.2.1 Analyzed referring to stress

The Kaiser effect is described as the absence of detectable acoustic emission at a fixed sensitivity level, until previously applied stress levels are exceeded. On the contrary, the presence of acoustic emission, which can be detected at a fixed predetermined sensitivity level at stress levels below those previously applied, which phenomenon is called Felicity effect[4]. During softening stage, it is impossible to load more than previously stress level (tensile strength), therefore, strictly speaking, does not exist Kaiser effect.

The stress value (F_u) corresponding to start further unloading in each loading cycles, and the stress value (F_r) corresponding to the time when AE signals begin to be detectable, are summarized in Tab. 3. It is can be found that, the values of F_r / F_u are less than 1 (Obviously, the ratio of F_r / tensile strength is also less than 1), so the Felicity effect also exists.

Specimen No.	Cycle	F_u(MPa)	F_r (MPa)	F_r/ F_u	ε_u(με)	ε_r(με)	ε_r/ ε_u
DT02	1th	1.152	1.015	0.881	154.234	153.325	0.994
DT03	1th	1.376	1.327	0.965	220.737	224.056	1.015
	2nd	1.266	1.192	0.941	252.109	251.810	0.999
	3rd	1.121	0.928	0.828	296.070	275.287	0.930
DT04	1th	1.184	1.135	0.959	177.858	176.646	0.993
	2nd	1.138	1.068	0.938	190.417	188.982	0.992
	3rd	1.062	1.032	0.972	216.389	218.438	1.009
	4th	0.940	0.860	0.914	254.625	244.775	0.961

Table 3. Acoustic emission Characteristics at the Unloading-reloading process in the softening portion

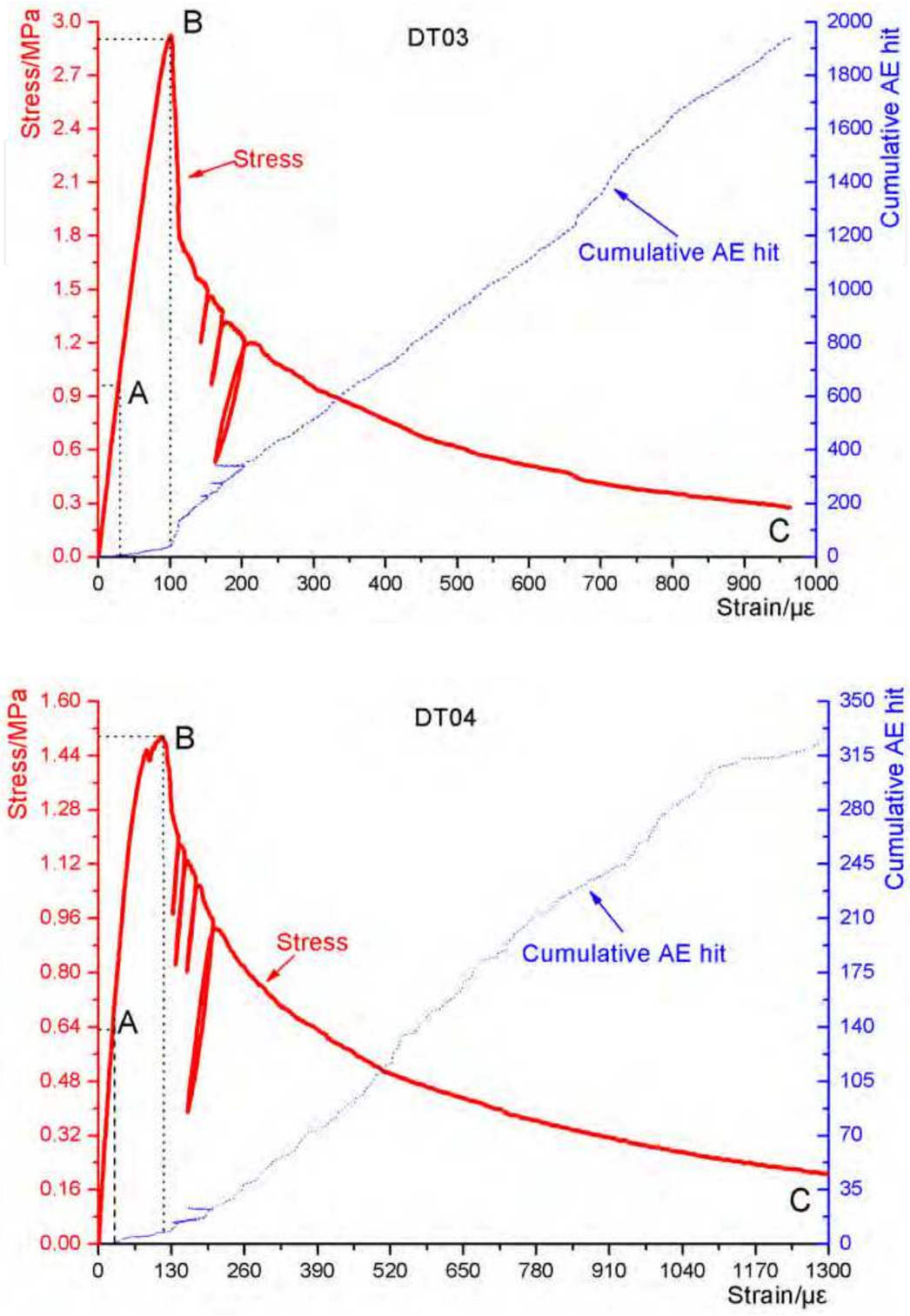

Fig. 5. Tensile stress and accumulated AE hit number versus strain

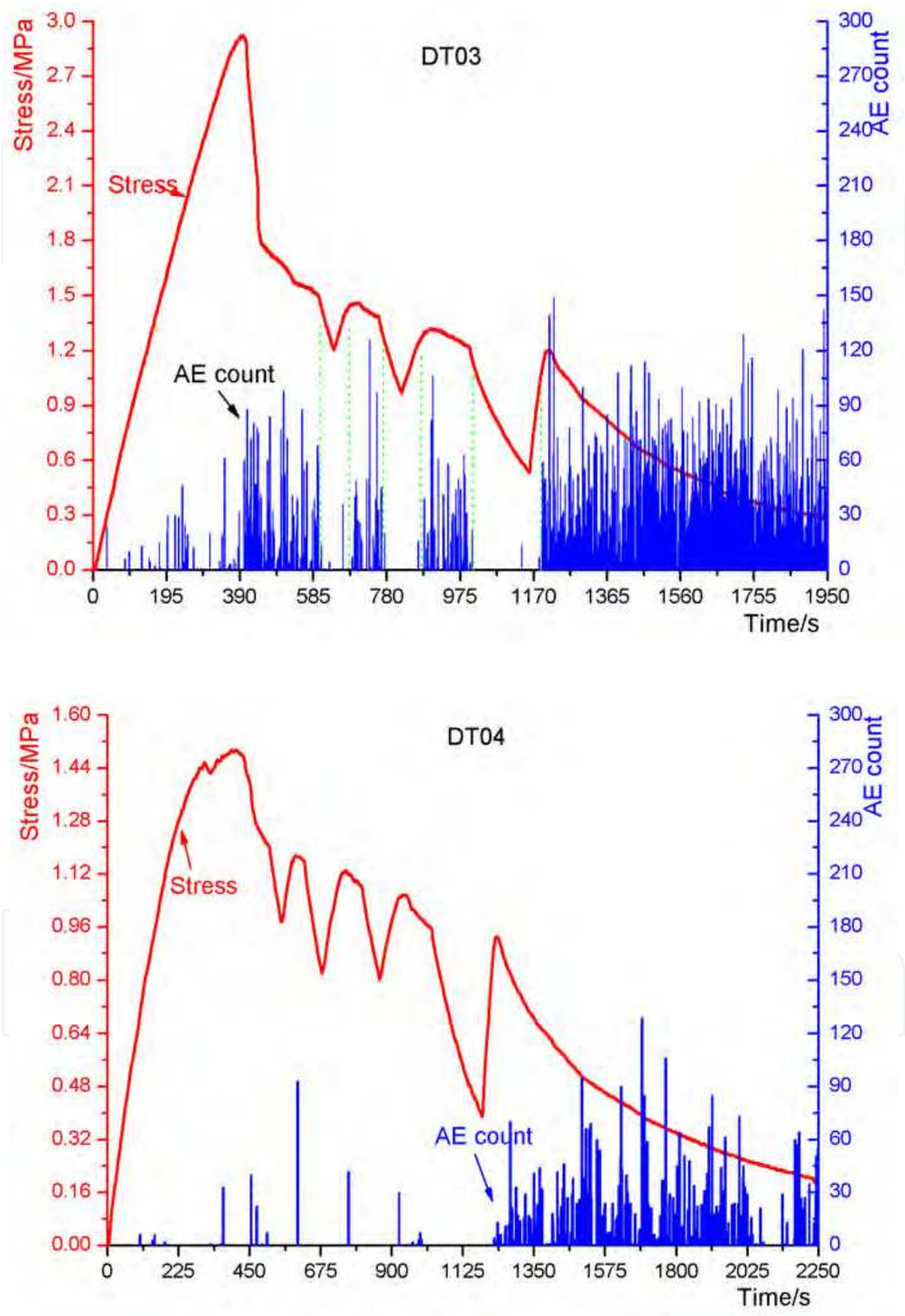

Fig. 6. Tensile stress and AE count number versus time

4.2.2 Analyzed referring to strain (Deformation)

It is can be seen from Figure 7, in the softening phase of the process of loading. The strain increased with the decreased loading (tensile stress), while the strain decreased when further unloading. The strain value (ε_u) corresponding to start further unloading in each loading cycles, and the strain value (ε_r) corresponding to the time when AE signals begin to be detectable, are summarized in Tab. 3. It can be found that, the value of $\varepsilon_r/\varepsilon_u$ during each cycles are around 1, and the value is decline in the last cycle. Hence the acoustic emission can still memory the maximum strain in the loading history, at the same time, the values of $\varepsilon_r/\varepsilon_u$ is larger than the value of F_r / F_u in each load-unloading cycle, therefore, the memory effect of strain of acoustic emission is better than the stress, it is maybe mainly due to the closed-loop servo system used the deformation from the specimens as a loading control signals.

The above properties during the soften stage maybe related to the stress states of concrete specimens: the cracks in the concrete are I-type, and they are mainly vertical to the loading direction. When entering the soften stage, the localized macro-crack has already formed. Then the single macro crack widens in concrete specimens, and there are no mutually dislocation activities. Therefore, there is no obvious AE phenomenon.

4.3 Spatial distribution of AE activities

The mechanical behavior before crack localization, which coincides with the peak stress, can be regarded as intrinsic to the material. That is, as the cracks are small with respect to the volume of the specimen, statistically homogeneous stresses and strains can be defined. Fig. 8 confirms that before the axial stress reaches the limits of stress (before 390 s), the cumulative AE hit curve described in different AE transducers located in different positions of the specimens have no obvious differences.

After localization, since these cracks are no longer assumed to be small with respect to the volume of the specimen, statistically-homogeneous stresses and strains cannot be defined. Therefore, the only relation is between the force and the displacement, which are both global parameters. The behavior is then structural, and this can also be confirmed in Fig. 8. In the soften stage of stress-strain curve, the AE hit number described by the transducer closest to the visible crack (visible crack can be seen in fig. 9) has maximum value. In addition, the locations of AE events calculated by the location method mentioned above and the position of visible crack are shown in Fig. 9. The AE events appear during the post peak stage of soften stage. It is found that most of the AE events are located close to the actual position of the visible crack. Same as the research results from Zongjin Li[13], the obvious microcrack localization phenomenon is observed. This phenomenon can be demonstrated through AE hit cumulative curve in the sensors located in different positions and AE source location technology.

From the stress-strain curves shown in Fig. 10, we can see that the final location of the crack is out of the resistance strain gauge in shorter length, but the crack is located in the range of extensometer. Therefore, the curves expressed by the two measurements are different, and this result can further explain the microcrack localization phenomenon.

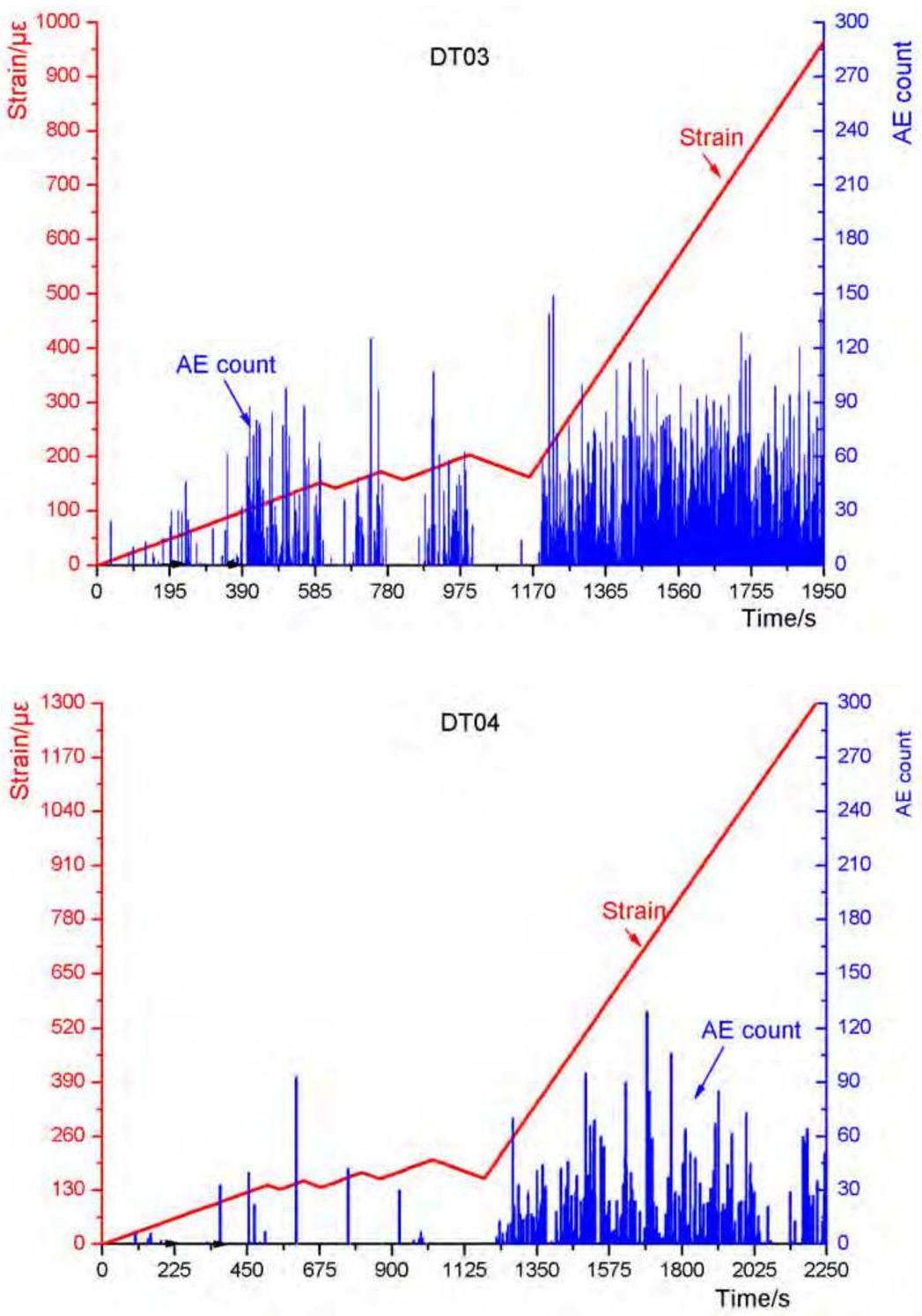

Fig. 7. Tensile strain and AE count number versus time

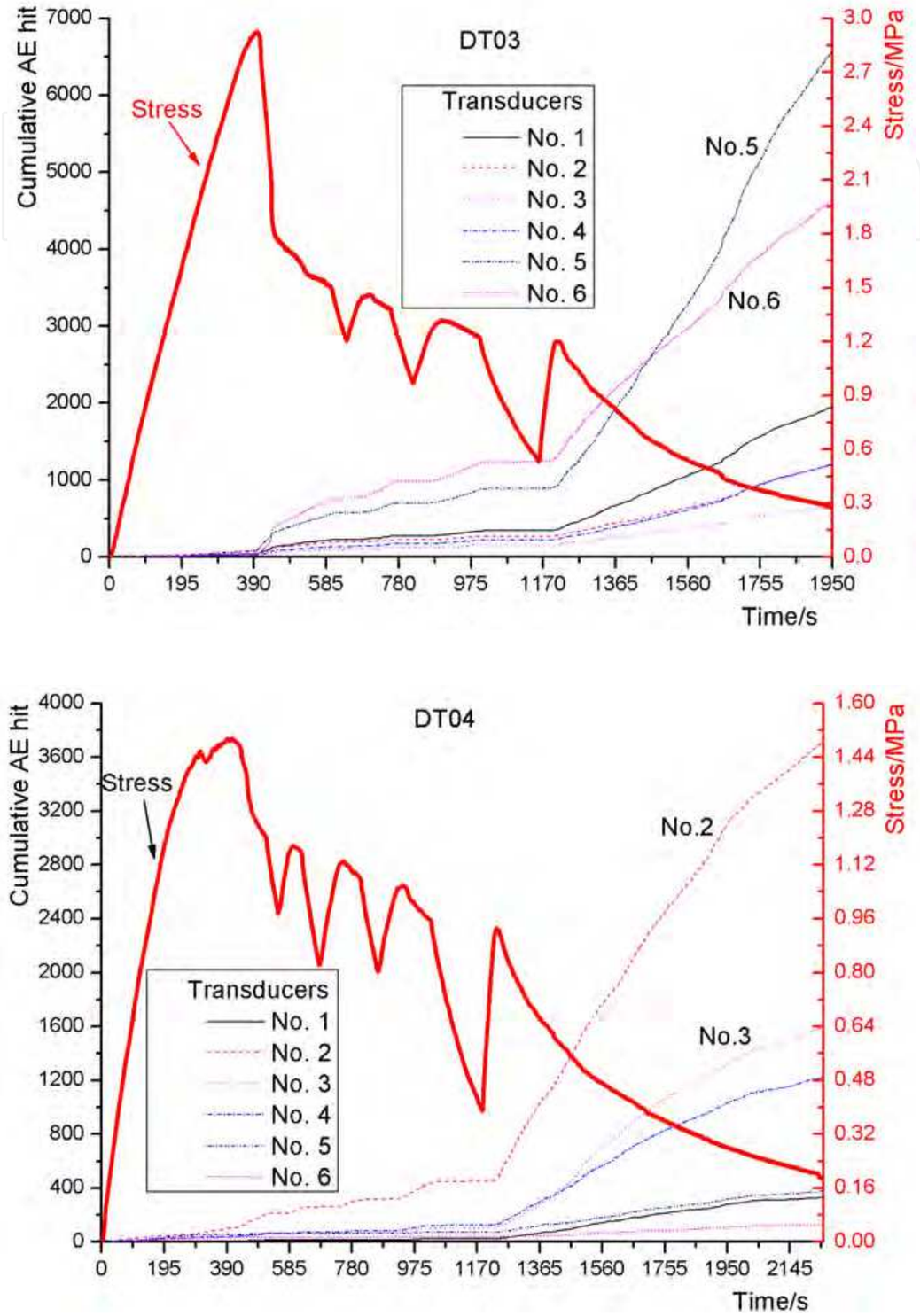

Fig. 8. Tensile stress and accumulated AE hit number versus time for different transducers

To summarize, the material switch to structural properties of concrete under Uniaxial tension can be understood as[9] follows: if the switch is thus performed with the macrocracks after localization, the relation will depend significantly on the positions of the macrocracks in the specimen, which is typical structural behavior.

4.4 AE parameter analysis

Compared to the previous stage, it can be seen from Fig. 11 to Fig. 12 that in the soften stage of concrete specimen under Uniaxial tension, as the crack further opens, AE hits in higher amplitude (greater than 60 dB) and longer duration (more than 600 μ s) are generated. This indicates that the energy released from microcracks tend to increase during the soften stage.

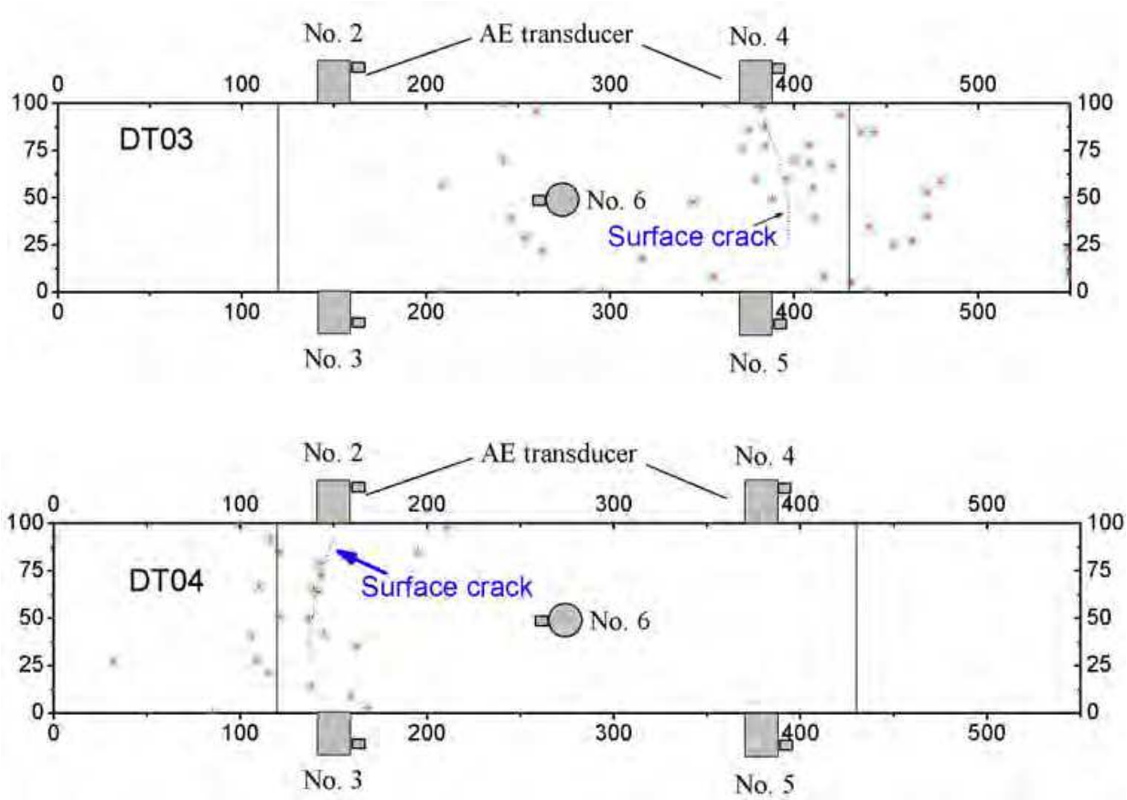

Fig. 9. AE source locations

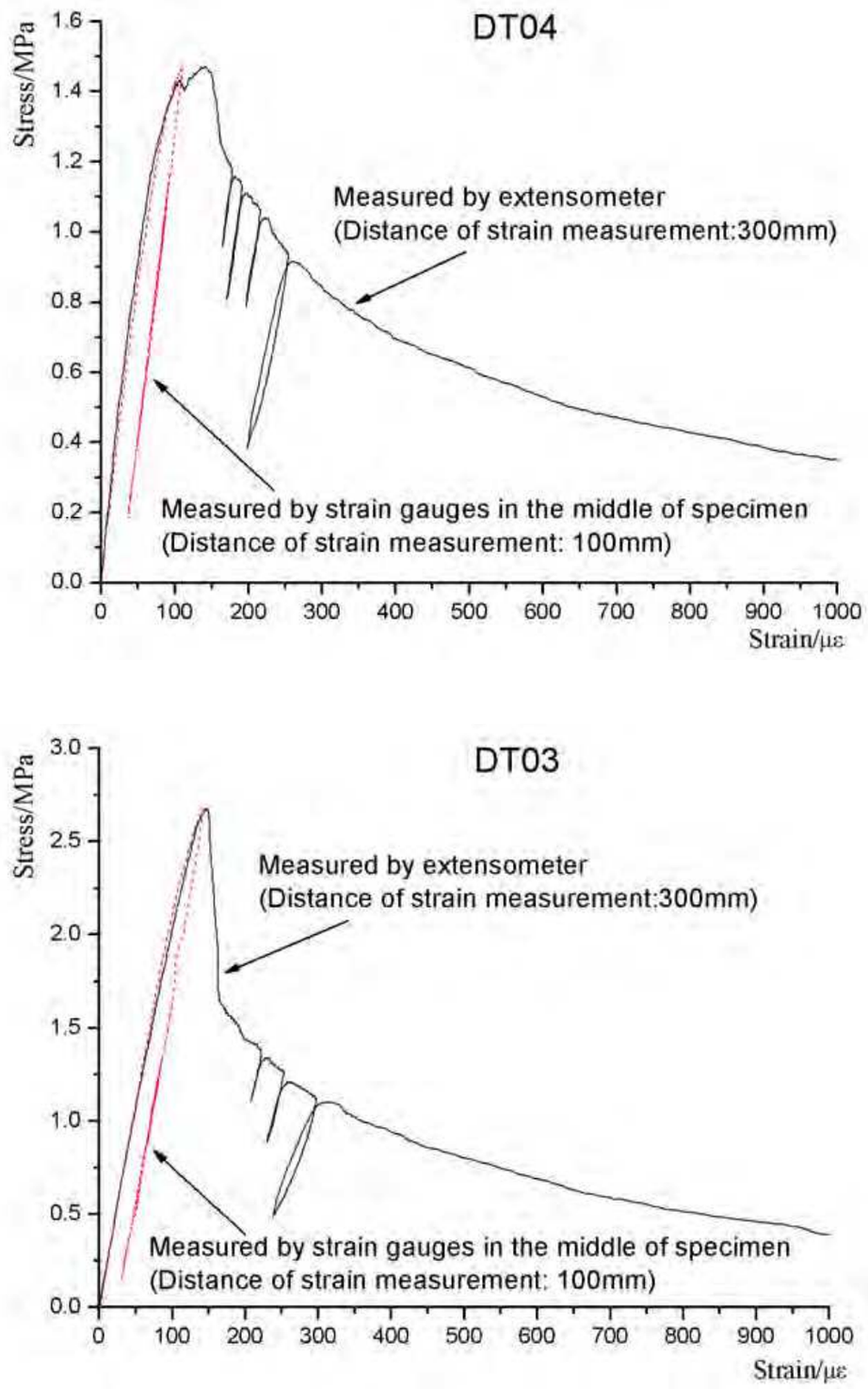

Fig. 10. Stress-strain relationships measured by extensometer and strain gauges

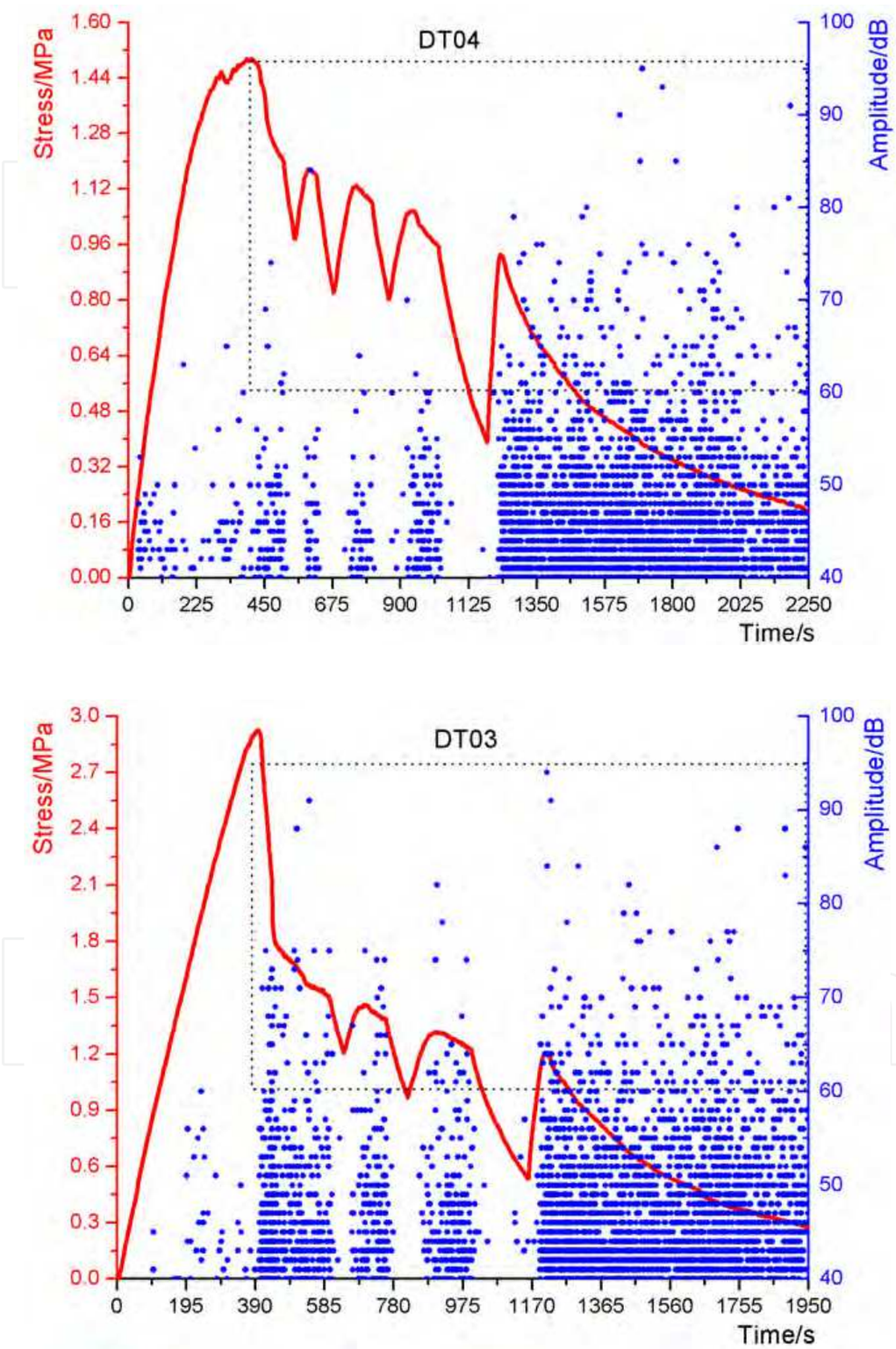

Fig. 11. Tensile stress and amplitude versus time

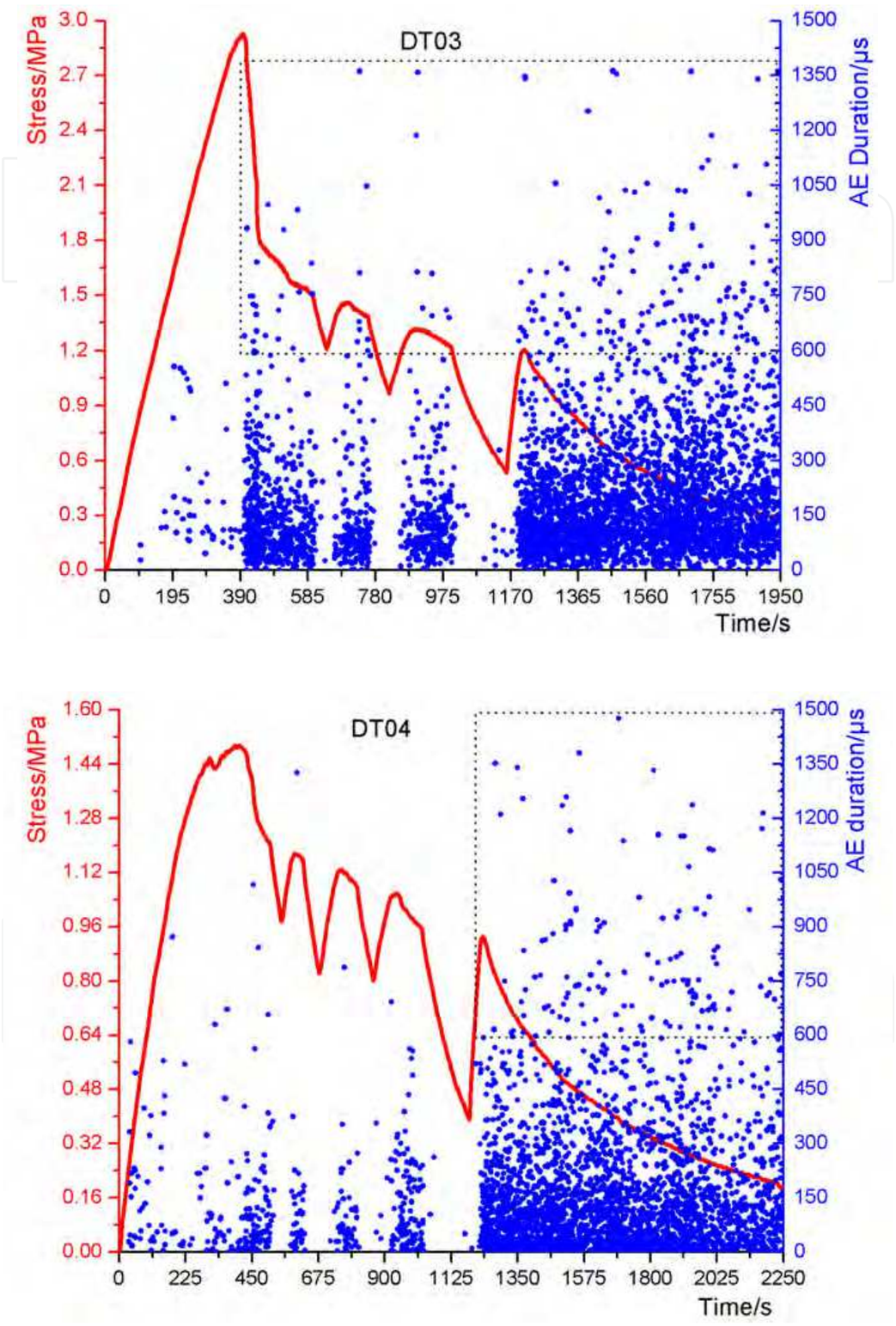

Fig. 12. Tensile stress and duration versus time

5. Conclusions

Through acoustic emission signal analysis of concrete specimens under Uniaxial tension, the AE characteristics of concrete in the whole process of tension are obtained. The conclusions are as follows:

1. Although the width of cracks are too small to be seen by naked eyes, and the specimens are not broken into two parts, the process of developing microcracks can be displayed and demonstrated in real time by AE technology.
2. Good relationship between acoustic emission hit rate and microcracks development in the concrete is found. Therefore, analysis of the timing characteristics of AE activities in concrete is helpful to assess the damage level.
3. During the deterioration stage of soften, unloading-reloading process cannot exceed the tensile strength of the specimen. The Kaiser effect, therefore, does not exist while Felicity effect exists.
4. The maximum strain can still be characterized by AE during the soften process of concrete, and the accuracy is higher than that of the stress memory effect.
5. Before the stage of microcrack localization, AE activities described by the sensors in different position of the specimens are close. No significant differences are observed. During the process of localization of microcracks to the formation of macrocracks, AE activity described by sensors is significantly different, materials-structural characteristics of concrete under Uniaxial tension are further confirmed.
6. AE activities from different sensors and the localization results of acoustic emission source are consistent with the actual distribution of visible crack.
7. The energy released from microcracks activities tend to increase during the soften stage, and AE hits in higher amplitude and longer duration are detected.

6. Acknowledgments

The authors appreciate the support of the National Natural Science Foundation of China (Grant No. 51178162 and Grant No. 51009058).

7. References

[1] Yang Weizhong, Wang Bo. A stochastic damage constitutional model and its application to uniaxial tensile behavior of concrete[J]. Industrial Construction. 2004, 34(10): 50-52, 43(in Chinese).

[2] Qian Jueshi, Wang Zhi, Luo Hui. Determination of strain softening relationship of concrete [J]. Journal of dalian University of technology. 1997, 37(1): S61-S66(in Chinese).

[3] Z. Li, S. M. Kulkarni, S. P. Shah. New Test Method for Obtaining Softening Response of Unnotched Concrete Specimen Under Uniaxial Tension [J]. Experimental Mechanics, 1993, 33(3): 181-188.

[4] ASTM E 1316-99a, Standard terminology for nondestructive examinations [S].

[5] M A Majeed, C R L Murthy. On using peak amplitude and rise time for AE source [J]. Sadhana. 2002, 27(3): 295-307.

[6] K. Malen, L. Bolin. A Theoretical estimate of acoustic-emission stress amplitudes [J]. phys. stat. sol. (b). 1974, 61(2): 637-545.

[7] WANG Yan, WU Sheng-xing, ZHOU Ji-kai, et. al. . 3D Acoustic Emission Source Location Based on Exhaust Method [J]. Nondestructive Testing. 2008, 30( ): ??-??. article in press. (in Chinese).
[8] Rossi, P., Wu, X.. A probabilistic model for material behaviour analysis and appraisement of the concrete structures [J]. Magazine of Concrete Research, 1992, 44 (161): 271-280.
[9] P. Rossi, F. Toutlemonde. Effect of loading rate on the tensile behaviour of concrete: description of the physical mechanisms [J]. Materials and Structures, 1996, 29: 116-118.
[10] Landis E.N. Micro-macro fracture relationships and acoustic emissions in concrete[J]. Construction and Building Materials. 1999, 13(1): 65-72.
[11] Li Z, Shah SP. Microcracking in concrete under uniaxial tension[J].ACI Materials Journal, 1994, 91: 372-381.
[12] Lu Yiyan He Shaoxi. Experimental Research on the Complete Stress-strain Curve with Hoop Tension for SFRC [J]. Journal of wuhan university of hydraulic and electric engineering. 1995, 28 (3): 285-292(in Chinese).
[13] Zongjin Li, Surendra P. Shah. Localization of Microcracking in Concrete under Uniaxial Tension [J]. ACI Materials Journal, 1994, 91(4): 372-381.

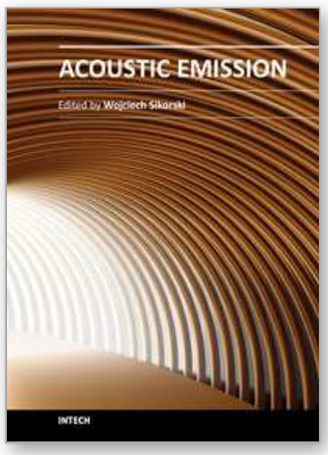

Acoustic Emission

Edited by Dr. Wojciech Sikorski

ISBN 978-953-51-0056-0
Hard cover, 398 pages
Publisher InTech
Published online 02, March, 2012
Published in print edition March, 2012

Acoustic emission (AE) is one of the most important non-destructive testing (NDT) methods for materials, constructions and machines. Acoustic emission is defined as the transient elastic energy that is spontaneously released when materials undergo deformation, fracture, or both. This interdisciplinary book consists of 17 chapters, which widely discuss the most important applications of AE method as machinery and civil structures condition assessment, fatigue and fracture materials research, detection of material defects and deformations, diagnostics of cutting tools and machine cutting process, monitoring of stress and ageing in materials, research, chemical reactions and phase transitions research, and earthquake prediction.

InTech Europe
University Campus STeP Ri
Slavka Krautzeka 83/A
51000 Rijeka, Croatia
Phone: +385 (51) 770 447
Fax: +385 (51) 686 166
www.intechopen.com

InTech China
Unit 405, Office Block, Hotel Equatorial Shanghai
No.65, Yan An Road (West), Shanghai, 200040, China
中国上海市延安西路65号上海国际贵都大饭店办公楼405单元
Phone: +86-21-62489820
Fax: +86-21-62489821

IntechOpen